Desalination and Water Treatment
www.deswater.com
doi: 10.1080/19443994.2015.1004596

57 (2016) 5498–5513
March

Taylor & Francis
Taylor & Francis Group

An ecofriendly approach towards remediation of high lead containing toxic industrial effluent by a combined biosorption and microfiltration process: a total reuse prospect

Animesh Jana[a,b], Priyankari Bhattacharya[a], Sandeep Sarkar[a], Swachchha Majumdar[a], Sourja Ghosh[a,*]

[a]*Ceramic Membrane Division, CSIR-Central Glass and Ceramic Research Institute, 196, Raja S.C. Mullick Road, Kolkata 700032, India, Tel. +91 33 2473 3469/76; Fax: +91 33 2473 0957; emails: janaaanimesh@gmail.com (A. Jana), priyankari2004@yahoo.co.in (P. Bhattacharya), sandeep@cgcri.res.in (S. Sarkar), swachchha@cgcri.res.in (S. Majumdar), sourja@cgcri.res.in (S. Ghosh)*
[b]*AcSIR-IMP, CSIR- Central Glass and Ceramic Research Institute, Kolkata, India*

Received 30 May 2014; Accepted 26 December 2014

ABSTRACT

An environment friendly approach involving biosorption, integrated with ceramic membrane-based microfiltration, was employed for treatment of high lead-containing printing industry effluent. Dried sludge from a common effluent treatment plant of a tannery was used for the preparation of a cost-effective biosorbent. The biosorption capacity for lead obtained was about 199 mg/g at pH 4.2 in a synthetic solution with initial lead concentration of about 1,000 mg/L. With a significantly high concentration of lead in effluent, i.e. about 1,000 mg/L, about 99% removal could be achieved using 5 g/L of biosorbent dose. Microfiltration study was conducted using indigenously developed ceramic membranes. The combined process resulted in 99.9–99.5% reduction of total organic carbon and chemical oxygen demand, respectively. The treated effluent was applied in agriculture by conducting the seed quality assessment test. It was observed that germination (%) of three types of seeds, viz. chickpea, soybean, and dry white peas on exposure to treated effluent was comparable to that of control. In the case of the untreated effluent germination, (%) decreased with increasing concentration, i.e. 5–25%. The treated effluent did not affect the protein content of the seeds as compared to the control. The spent biosorbent was utilized for manufacturing of bricks. About 30% of the spent biosorbent in clay could be used to prepare bricks with reasonable compressive strength. The overall study indicated potential of the integrated process with complete recycling approach with respect to a toxic industrial effluent.

Keywords: Lead removal; Printing industry effluent; Biosorption; Microfiltration; Ceramic membrane; Reuse

1. Introduction

Several industries dealing with electroplating, paper and pulp, printing, textiles, etc. Discharge effluents that are highly contaminated with heavy metals, which impart significant toxicity in the environment. The metals are usually present in ionic forms which are nonbiodegradable, persistent, and difficult to remove [1]. These contaminants enter the human

*Corresponding author.

body through the food chain causing serious damage to health as well as the ecological balance. Often the small-scale industries fail to follow the stringent rules for discharge limits of effluents due to lack of suitable remediation technologies. Lead, used widely in industries like printing, pigment, photographic, and explosives, is one of the most dangerous nonferrous metals. Toxicity of lead is expressed in very low concentrations. Thus, the recommended limit for lead in drinking water is about 0.01 mg/L according to the World Health Organization (1984). In the printing industry, lead is commonly used as an alloy containing tin and antimony [2], and the effluent contains high concentration of lead. Workers of these industries are often exposed to occupational health hazards due to lead toxicity. Exposure to lead causes disorder in the nervous system and brain [3]. Thus, many processes are being undertaken for removal of the metal ions from the effluent. Some common processes are chemical precipitation, ion-exchange, reverse osmosis, adsorption, solvent extraction, etc. [4]. Adsorption is widely used for treatment of wastewater as well as for removal of toxic heavy metals. Due to the high cost of activated carbon, various types of biomass like agricultural wastes, dried sludge, fruit peels, etc. are being used. Wilson et al. reported the adsorption capacity of activated carbon prepared from peanut shells for selective metal ions like cadmium, nickel, lead, copper, and zinc [5]. Gong et al. studied the removal and recovery of lead from aqueous solution using intact and pretreated biomass of *Spirulina maxima* [6]. It has been observed that use of dead biomass like driedactivated sludge provides equal or more adsorption of heavy metal. Cell surface of bacteria is anionic in nature because of the ionized group present in cell wall polymer. This results in attraction of cationic metal groups. Moreover, dead biomass reduces the toxicity problems associated with living biomass as well as eliminates use of nutrients required for growth of biomass [7]. Dried activated sludge has been investigated for cadmium biosorption which showed that using a dose of 2 g/L resulted in 79% removal of cadmium [8].

The adsorption process proves to be efficient for removal of heavy metals and selective components. However, several other contaminants exist in industrial effluent, including a large content of suspended solids, oil and grease, and various other inorganic and organic materials, which are difficult to remove by biosorption alone. In view of this, an integrated process was proposed in the present study, involving biosorption followed by membrane filtration for treatment of a concentrated effluent from printing industry sector containing high content of lead, TOC, COD as well as oil and grease. Dried sludge was collected from a common effluent treatment plant of tannery industry and this waste biomass was utilized for removal of lead after necessary surface treatments. Biosorption behavior of the prepared biosorbent was observed using synthetic lead solutions. The mechanism of biosorption was studied with the help of various characterizations, viz. XPS, XRF, FESEM, XRD, pzc, and FT-IR. Biosorption equilibrium data were fitted to two- and three-parameter isotherm model equations available in the literature. Desorption behavior of the spent biosorbent was observed using different reagents.

Ceramic microfiltration membranes, indigenously prepared from an optimum composition of clay and alumina [9], were used in combination with the biosorptive treatment with an objective of complete recycling of the effluent. In an earlier study, such a process resulted in an effective removal of COD, dyes as well as other suspended and turbid contaminants from industrial effluent [10,11]. In the current work, the effect of operating pressure on permeate flux was studied at constant cross-flow velocity. Flux profile with time was monitored at constant (TMP). The experimental flux data were fitted to standard models for flux decline and the effluent was characterized in detail at different stages of treatment.

The feasibility of reusing the treated effluent in agriculture was explored by conducting seed germination tests using three different kinds of seeds. Effect of industrial effluents on germination of various seeds such as *Sorghum vulgare* (Jowar) and *Vigna aconitifolia* (Matki) has been observed by Panaskar and Pawar [12]. They subjected the seeds to various concentrations of effluent in the range 20–100% along with distilled water as control. Various parameters like seed germination, mean root lengths of germinated seedlings, plumule germination, mean plumule length of germinated seedlings, disease (fungus), etc. were observed. In an earlier study, phytotoxicity of Cr^{+6} was analyzed by studying the seed germination behavior and enzyme activity of a pulse seed (*Vigna radiata* L.), which showed that biosorptive treatment could effectively remove Cr^{+6} from aqueous phase, thereby leading to considerable enhancement of seed germination as well as increase in root length [13]. In the present work, the effect of the seed germination characteristics including germination rate, root and shoot length, seedling vigour index, protein content, etc. was studied with respect to the treated effluent. Results were compared to those using the control as well as the untreated effluent in various dilutions.

Finally with an objective of waste to value-added product generation, the spent biosorbent was mixed

with clay in different proportion for the preparation of bricks [14]. The brick samples were sintered at 1,000˚C. Density and compressive strength of the brick samples were measured to arrive at the optimum composition. Subsequently, the brick samples were studied for their leaching behavior in an extreme condition.

2. Materials and methods

2.1. Collection and characterization of effluent

The effluent was collected from a reputed printing industry located in Kolkata, India. Lead concentration of the effluent was measured using atomic absorption spectrophotometer (Perkin Elmer, USA). In addition, the wastewater was subjected to characterization in terms of chemical oxygen demand (COD), biochemical oxygen demand (BOD), turbidity, total solids, total dissolved solids (TDS), conductivity, total kjeldahl nitrogen (TKN), total organic carbon (TOC), pH, oil and grease content, etc. All analytical work was done as per methods described in APHA [15]. The chemicals used for the experiments were from Merck, GR, India. COD was analyzed by dichromate reflux method in a COD digester of Spectra lab, India and a BOD Track apparatus (HACH, USA) was employed for BOD by measuring the depletion in dissolved oxygen level using the five d BOD technique. The other parameters like TDS, turbidity, pH, and conductivity were analyzed in instruments by HACH, USA. TKN was analyzed using KJEL PLUS block digestion system with semi-automatic distillation unit (Pelican Instruments, India). For TOC measurement, TOC-V combustion-type model of shimadzu was used based on 680˚C combustion catalytic oxidation method. The oil and grease content of effluent samples was analyzed by partition-gravimetric method (APHA) and color intensity of samples was measured using UV-vis spectrophotometer of Varian, Australia.v

2.2. Preparation of biosorbent

Dried sludge was collected from a common effluent treatment plant of tannery industry. Immediately after collection, the sludge was powdered and sieved through 200 μm mesh. The powdered sludge was subjected to alkali treatment using different strengths of sodium hydroxide solution, i.e. 0.00025–0.05 M for a contact time of 3 h under stirring speed of 300 rpm. The treated biomass was thoroughly washed with distilled water until the washed water was alkali free. The biosorbent was then subjected to autoclaving at 15 lbs pressure and 120˚C for 20 min for surface activation [16]. The biosorbent thus prepared was oven dried at 80–90˚C for 24 h. It was then powdered and sieved though 150 μm mesh and kept in airtight container.

2.3. Characterization of biosorbent

Surface morphology and microstructure of the biosorbent were observed using field emission scanning electron microscopy (FESEM, Zeiss, Germany). In addition, elemental composition of the biosorbent was studied by energy-dispersive X-ray analysis (EDX) at different spots of the biosorbent before and after sorption. For identification of various functional groups and related active sites, Fourier transform infrared spectroscopy (FT-IR, Perkin Elmer, USA) was undertaken within a range of 400–4,000 cm^{-1}. Surface area of the biosorbent was measured by multipoint BET method from N_2 adsorption/desorption isotherm using Autosorb-1 (Quantachrome Instruments, USA). The point of zero charge (pzc) was determined using zeta potential analysis of the biosorbent in Zetasizer of Malvern Instruments, UK, for understanding the interaction between the adsorbate and the biosorbent. For structural analysis and identification of the phases of different components present in the biosorbent, powder X-ray diffraction was carried out using Philips 1,710 diffractometer with CuK_α radiation ($\alpha = 1.541$ Å), where X-ray patterns were observed in the 2θ range between 5 and 90˚. Thermogravimetric analysis was undertaken to understand the thermal stability of the biosorbent under combustion atmosphere with a heating rate of 5˚C/min using TGA NETZSCH instrument (Germany). For elemental analysis of the biosorbent in solid phase before and after sorption, XRF was performed using X-ray fluorescence spectrometer (Axios, PANalytical, The Netherlands). To understand the oxidation states of adsorbed lead in the surface of the biosorbent and identifying the bonding nature of the chemisorbed lead, X-ray photoelectron spectroscopy technique was employed using PHI 5000 XPS-analyzer, Versaprobe-II, USA. Other characterization methods included analysis of chemical compositions of the biosorbent before and after sorption using atomic absorption spectrophotometer (Perkin Elmer, USA), porosity measurement by mercury intrusion technique up to 345 MPa pressure range (Quantachrome Poremaster, USA), and determination of organic matter, bulk density, moisture content, ash content, etc. Various physicochemical characteristics of the biosorbent are shown in Table 1.

Table 1
Characteristics of surface activated dried biosorbent

Parameters	Values
Surface area (m^2/g)	14.2
Ash content (%)	42
Moisture content (%)	4.5
Bulk density (g/cc)	0.63
Particle size (μm)	140
Organic matter (% by weight)	3.5
Porosity (%)	38
Isoelectric point	4.1

2.4. Batch biosorption study with synthetic lead solution and effluent

Biosorption study was conducted in batch mode with synthetic solution of lead. Stock solution of 1,000 mg/L was prepared by dissolving pure lead nitrate in distilled water. Since a high concentration of lead (1,000–1,200 mg/L) was found in the industrial effluent, the effects of pH and biosorbent dose were observed in synthetic media with a similar value of initial lead concentration of about 1,000 mg/L. For pH optimization, initial pH of the solution was varied from 2.0 to 5.0 using 5 g/L of biosorbent dose. The sample was stirred at 200 rpm for 22 h and temperature was maintained at 30°C. The effect of biosorbent dose was studied in the range of 0.5–7.0 g/L at an optimum pH of 4.2 keeping all other parameters constant. The equilibrium isotherm studies were conducted at three temperatures of 10, 30, and 50°C with initial concentration of 10–1,000 mg/L using biosorbent dose of 5 g/L and pH 4.2. Effect of contact time on lead removal was observed using two different initial concentrations of lead solution, i.e. 500–1,000 mg/L at 30°C and at a high stirring speed of 1,000 rpm. The biosorption capacity (q, mg/g) was calculated using the well-known equation,

$$q = V\ (C_0 - C_t)/m_a \quad (1)$$

where C_0 (mg/L) is the initial lead concentration in the solution and C_t (mg/L) was the lead concentration at any time t, V is the solution volume (L), and m_a was the biosorbent mass (g).

Based on the previously optimized value of the dose, pH, and temperature, about 10 L of effluent was treated with the biosorbent for further studies using the microfiltration process.

2.5. Microfiltration study

The biosorbent treated effluent was further subjected to microfiltration treatment using indigenously developed ceramic membranes. The clay-alumina-based membrane elements were tubular having an inner diameter of 3 mm, outer diameter of 5 mm, and an effective length of 150 mm. Porosity of the membrane was 36% with an average pore size of around 1 μm. The membrane module consisted of nine such membranes encased in a housing made of poly(methyl methacrylate) which was horizontally aligned in the setup. A 20 L capacity stainless steel make cylindrical tank with water cooling jacket was used as the feed tank. For liquid recirculation, a 2HP feed pump was used and the liquid flow rate was observed by a flow meter (0–35 L/min). The temperature of the feed was kept at 25°C during the membrane study. The effect of the operating pressure was observed in microfiltration using different transmembrane pressure ranging from 0.02–0.2 MPa with a constant cross-flow velocity of 1.6 m/s. Finally, at constant pressure of 0.098 MPa and cross-flow velocity of 1.6 m/s, filtration was carried out for 5 h. Permeate samples were collected at regular intervals for detail characterization. After each study, the setup was thoroughly cleaned by recirculating deionized water repeatedly at low pressure with high feed velocity followed by washing with 0.1 N hydrochloric acid. Then the module was again washed with deionized water successively after which the permeability of the clean membrane could be restored close to that of the fresh membrane.

2.6. Reuse study with the treated effluent

To observe the applicability of treated effluent for agricultural purpose, seed quality germination study was conducted using different concentrations of the untreated effluent and the results were compared with that using the treated effluent produced by the proposed process. Three different pulses with high protein content and nutrition value were selected for seed quality assessment which was *Cicer arietinum* L. (chickpea), *Glycine max* (L.) Merr. (soybean), and *Lathyrus sativus* L. (dry white peas). Uniform-sized certified packaged seeds were purchased from local market. The seeds were subjected to surface sterilization in 0.1% (w/v) mercuric chloride solution and then rinsed thoroughly using sterilized distilled water for about three times. Seeds were then transferred to a sterilized petri dish of 5 cm diameter containing sterilized filter paper (Whatman 42). About 10 seeds in triplicates were taken and placed in the filter paper. The seeds were then subjected to five different types of treatments, i.e. *T*1 (Control), *T*2 (treated effluent), *T*3 (5% effluent), *T*4 (10% effluent), and *T*5 (25% effluent). It was observed that in higher concentration

of effluent, i.e. 50% effluent, seeds became soggy and were rotten. Hence experiments were conducted with the above five treatments. The petri dishes were then placed in seed germinator in dark (Yorco Y58765, India) and maintained at 25˚C. Germination behavior of the seeds was observed after each 24 h up to 72 h. For seed quality assessment, several parameters were analyzed like germination (%), root length, shoot length, seedling length, seedling vigour index, seedling dry weight, speed of germination and first count of germination, protein content, etc.

Germination test (%) was conducted as per the method described in ISTA rules (Anonymous, 1999). The total germination was calculated from the daily germination counts and expressed in percentage. Shoot length was measured from primary leaf to base of hypocotyl and mean shoot length was measured on the final day and expressed in millimeters. Root length of the seedlings was measured and expressed in millimeters. Adding the shoot and root lengths of the seedlings, the seedling length was calculated and expressed as mean seedling length (mm). Seedling vigour index was computed and expressed as a number by adopting the following formula as suggested by Abul-Baki and Anderson [17].

$$\text{SVI} = \text{Germination } (\%) \times \text{Seedling length (cm)}$$

For obtaining seedling dry weight (g/10 seedlings), the seedlings used for shoot and root length measurement were put in butter paper pockets and kept in an oven maintained at 100 ± 2˚C for 24 h. After drying, the seedlings were kept in desiccators for cooling. The weight of dried seedlings was recorded and means dry weight was expressed in milligrams [18]. Speed of germination is the summation of the number of seeds germinated on each day divided by respective day on which seedlings were counted and removed [19]. The Bartlett's germination rate index was calculated by using the following formula [20] represented as Eq. (2):

$$\text{GRI} = \frac{G1}{T1} + \frac{G2}{T2} + \frac{G3}{T3} + \frac{G4}{T4} \quad (2)$$

where $G1$, $G2$, $G3$, and $G4$ are germination (%) at 1, 2, 3, and 4th day of germination, respectively. The number of normal seedlings emerged on the day of first count of germination as per ISTA Rules was recorded and expressed as first count of germination (%) [21].

The mean data were statistically analyzed and subjected to the analysis of variance by adopting the appropriate methods as outlined by Panes and Sukhtame [22].

2.7. Desorption study

Desorption study was conducted using 0.1 M sodium chloride, 0.1 M acetic acid, and 0.1 M calcium chloride solution [23]. About 0.5 g of spent biosorbent was taken in 100 ml of each solution and the mixture was stirred for 120 min at 30˚C and 200 rpm. Samples were collected after 30 and 60 min, and lead concentration was measured.

2.8. Utilization of spent biosorbent

The large amount of biomass generated from the treatment process may be utilized in many applications like structural bricks for house building. To explore this, spent biosorbent was mixed with clay in varying compositions of 10, 20, 30, and 40%. The prepared mixture was compressed under 3 MPa pressure and brick-shaped pieces were cut. These samples were dried at 100˚C for 24 h and then incinerated at 1,000˚C temperature. Density and compressive strength of the prepared samples were measured. Compressive strength of the fired bricks was measured using AIMIL hydraulic press. The bricks were then subjected to compressive test for evaluation of mechanical properties. Leaching behavior of the brick samples was studied by submerging the samples in an acidic medium of pH 4.3 considering an extreme environmental condition like acid rain. After an uninterrupted contact for seven days in the acidic medium, the brick samples were separated and pH of the solution was adjusted at two with 1 N nitric acid so that no precipitate remains in the solution. The solution was then filtered and analyzed in AAS for measurement of lead, chromium, and copper.

The scheme of the entire experimental work is shown in Fig. 1.

3. Results and discussion

3.1. Characterization of biosorbent

XPS analysis of the biosorbent was performed to understand the probable mechanism of lead biosorption. The analysis of prepared biosorbent before and after biosorption from synthetic lead solution is depicted in Fig. 2. It was observed that after biosorption of lead there was peaks around 137.6 and 142.4 eV which corresponded to 4f7/2 and 4f5/2 of Pb (II) and the doublet separation between them was 4.8 eV. This binding energy at 137.6 eV corresponded to the binding energy of Pb in PbO [24] and Pb $(CH_3COO)_2$. The XPS peak of O1s at 529.7 eV corresponded to the metal-oxygen bond [25]. It was also

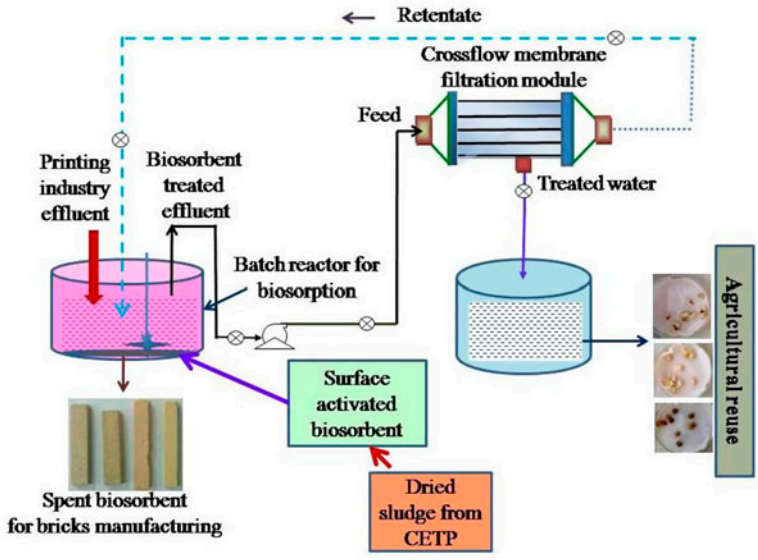

Fig. 1. The scheme of experimental work involving effluent treatment and reuse.

observed that peaks at 283.2 and 288.1 eV corresponded to C1s in C–H or C–C bond and C=O, respectively [26].

FT-IR analysis of the biosorbent is shown in Fig. 3. It is seen that there are peaks in the region of 3,400, 2,920, 1,660, 1,450, 1,080, 1,040, 870, 715, and 550 cm^{-1}. These represent –OH stretching of –COOH as well as water and –NH stretching of amines, –CH stretching of alkanes, C=O stretching, symmetric COO– stretching, C–N stretching, C–OH and C–O–C stretching of polysaccharides, phenyl ring substitution band (bending), –NH wagging, and $–SH_2$ and PO_4, respectively, in untreated biomass, surface-treated biosorbent, and biosorbent after use. It was observed that after surface treatment of the biomass, the intensity of symmetric stretching of COO– as well as that of C–OH and C–O–C stretching of polysaccharides increased. Increase in intensity of –NH wagging was also observed. After biosorption of wastewater, it was observed that intensity of symmetric COO– stretching decreased followed by decrease in intensity of –OH stretching of –COOH and –NH stretching of amine [27].

FESEM analysis revealed that there was no significant micro structural change in surface-treated biosorbent as compared to untreated biomass (Fig. 4(a)–(b)). After biosorption (Fig. 4(c)), it was observed that particles were deposited on the surface of biosorbent causing densification of the biosorbent surface. EDX analysis (Fig. 4(a)–(c)) revealed that there was no peak of lead before biosorption, while after biosorption a prominent peak of lead (~2.6 wt.%) was observed. The relative weight (%) of carbon and oxygen significantly changed after surface treatment of sludge and after biosorption when compared to untreated biomass.

XRD analysis (Fig. 5) showed that the peak (a) corresponded to $CaCO_3$ [27], whose intensity increased after surface treatment and decreased after biosorption of effluent. Interestingly, the intensity of the peaks (a) decreased slightly with respect to surface activated biosorbent after biosorption of synthetic lead. The reason might be attributed to the fact that in case of effluent presence of organic matter and other ions resulted in masking of $CaCO_3$ which was not prevalent in case of synthetic solution. Peaks at 26.9˚ corresponded to SiO_2 (b) and $C_4H_{10}O_7Pb_2$ (d) in the biosorbent after biosorption of effluent and synthetic lead solution. In case of synthetic lead solution, peak at 24.6˚ corresponded to $Pb(OH)_2$.

Quantitative XRF analysis was performed on the biosorbent before use and biosorbent after sorption with synthetic lead solution and effluent. The results shown in Table 2 indicate that the solid-phase concentration of lead was found to be about 190 mg/g, which was close to the experimentally obtained data of 199 mg/g measured with respect to the liquid-phase concentration values for lead solution having initial concentration of 1,000 mg/L.

TGA analysis of surface-treated sludge showed about 4% weight loss due to surface moisture elimination at 105˚C. Weight loss up to 320˚C was due to the entrapped moisture within the biosorbent. Further weight loss up to 530˚C was due to the degradation of organic matter present in the biosorbent (Fig. 6). This study indicated that the prepared biosorbent would be

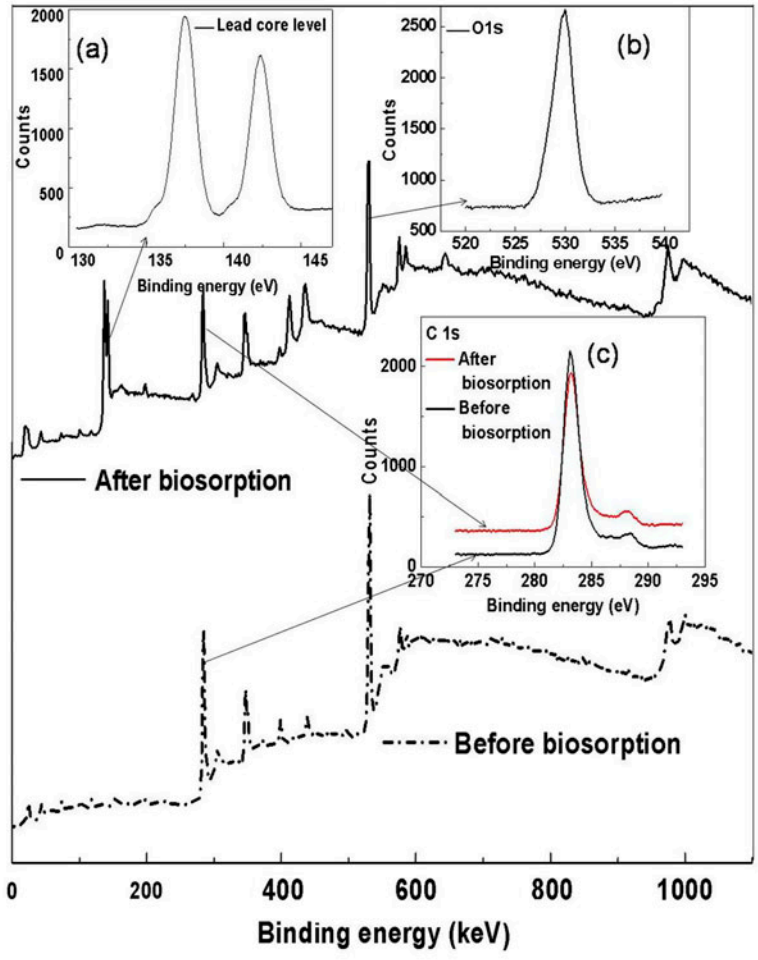

Fig. 2. Surface and core-level XPS analysis of biosorbent before and after biosorption. (a) Core level spectra of Pb 4f7/2, (b) core-level spectra of O 1 s, and (c) core-level spectra of C 1 s.

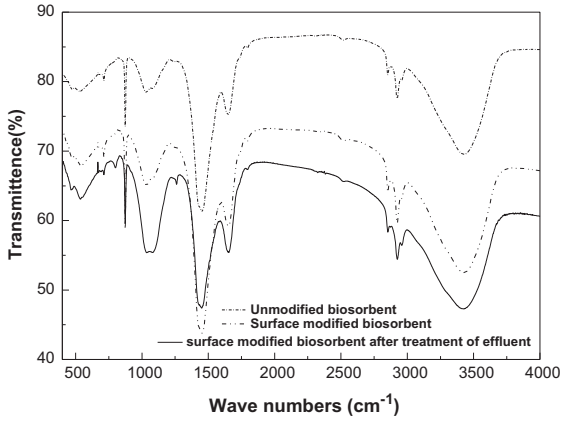

Fig. 3. FT-IR analysis of biosorbent before surface activation, after surface activation, and after biosorption of lead from effluent.

suitable for industrial-scale applications of effluent treatment.

3.2. Effect of pH in the biosorption of lead

The removal efficiency of Pb^{2+} was found to be highly dependent on the initial solution pH. The pH affects the surface charge of the biosorbent as well as the degree of ionization and speciations of the adsorbates are also affected [28]. The maximum removal was obtained at pH 4.2 (Fig. 7). The removal efficiency decreased as the pH increased to above 4.2. About 199 mg/g of biosorption capacity was obtained using 5 g/L of biosorbent dose. At a lower pH (<4.0–4.2), the biosorbent surface became positively charged due to higher H^+ ions concentration. Therefore, the repulsion took place between positively charged biosorbent and positively charged Pb^{2+} resulting in lower

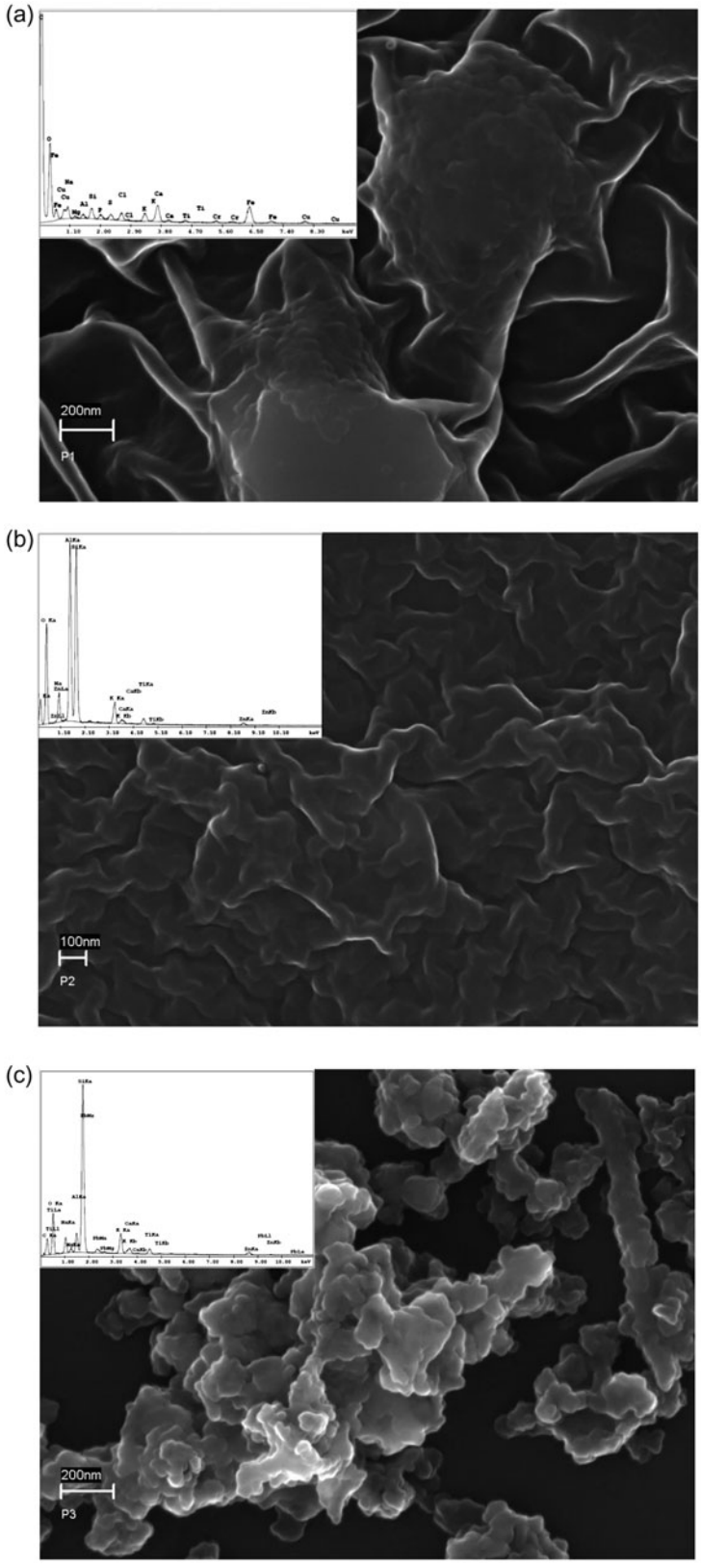

Fig. 4. FESEM and EDX of (a) biosorbent before surface activation, (b) biosorbent after surface activation, and (c) biosorbent after biosorption of lead.

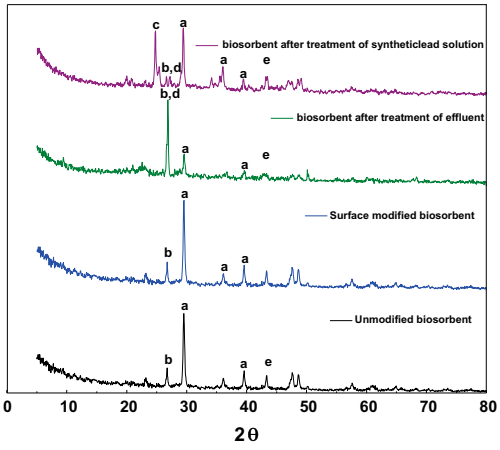

Fig. 5. XRD analysis of biosorbent before surface activation, after surface activation, after biosorptive treatment of effluent and after biosorptive treatment of synthetic lead solution; (a) $CaCO_3$, (b) SiO_2, (c) $Pb(OH)_2$, (d) $C_4H_{10}O_7Pb_2$, and (e) αAl_2O_3.

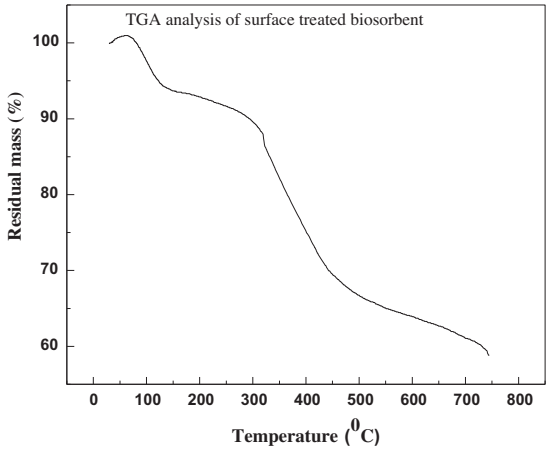

Fig. 6. TGA analysis of the surface-modified biosorbent.

biosorption capacity. From zeta potential analysis, the isoelectric point of the biosorbent was found to be about 4.1. Since at pH 4.2 the surface of the biosorbent became negatively charged, strong electrostatic attraction existed between the biosorbent surface, and Pb^{2+}. Above this pH, precipitation of Pb^{2+} occurred and therefore, biosorption experiments could not be performed. Similar results were observed by other researchers [29].

3.3. Effect of biosorbent dose in the removal of lead

Effect of biosorbent dose on Pb^{2+} removal was shown in Fig. 7, which indicated that biosorption of Pb^{2+} increased with increase in the biosorbent dose. The reason might be due to availability of active sites and effective surface area of the biosorbent. At equilibrium, the biosorption capacity decreased with increasing biosorbent concentration. An optimum dose of 5 g/L was considered for rest of the study.

Table 2
XRF data of untreated and treated biosorbent

	Compound name	Composition (wt.%) (before biosorption)	Composition (wt.%) (after biosorption)
1	Na_2O	0.330	0.327
2	MgO	1.896	1.786
3	Al_2O_3	8.220	6.076
4	SiO_2	15.254	20.332
5	K_2O	0.544	0.612
6	CaO	53.070	35.005
7	Cr_2O_3	15.157	14.782
8	MnO	0.891	0.56
9	Fe_2O_3	4.637	2.927
10	CuO	–	0.120
11	PbO	–	17.474

3.4. Effect of temperature on biosorption

From Fig. 8, it is seen that the biosorption capacity increased significantly as the temperature was increased from 10 to 50°C. Further it was observed that at a lower range of initial concentration, i.e. up to 100 mg/L, the biosorption capacity was not much affected by temperature and showed a significant effect at higher concentration (>100 mg/L).

From the equilibrium isotherm study at different temperatures, thermodynamic parameters such as standard Gibbs free energy change (ΔG°), standard enthalpy change (ΔH°), and standard entropy change (ΔS°) were estimated. The standard Gibbs free energy change was calculated using Eq. (3):

$$\Delta G^0 = -RT \ln K_C \tag{3}$$

where $K_c = C_{ae}/C_e$, is the equilibrium constant, C_{ae} (mg/L) is the amount of Pb(II) adsorbed in the biosorbent per liter of the solution at equilibrium and C_e (mg/L) is the equilibrium liquid-phase concentration of Pb(II). R is universal gas constant, which has a value of 8.314 J/mol K and T is the temperature in absolute scale. Standard enthalpy change (ΔH°) and standard entropy change (ΔS°) may be calculated from the slope and intercept of the plot of ln K_c vs. $1/T$ using Eq. (4):

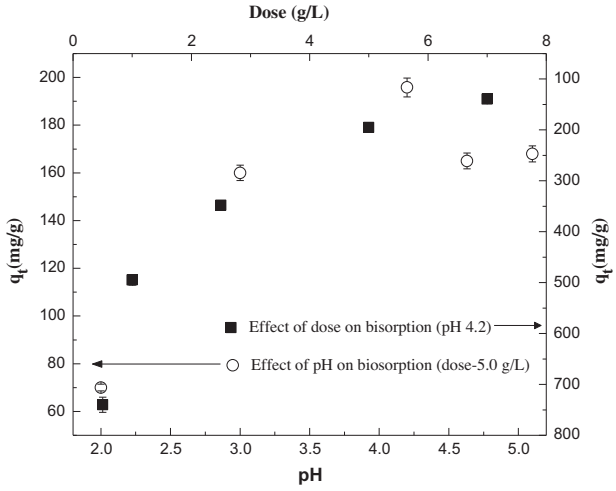

Fig. 7. Effect of varying dose and varying pH on biosorption of lead in a synthetic 1,000 mg/L lead solution; contact time 22 h, stirring speed 200 rpm, and temperature 30°C.

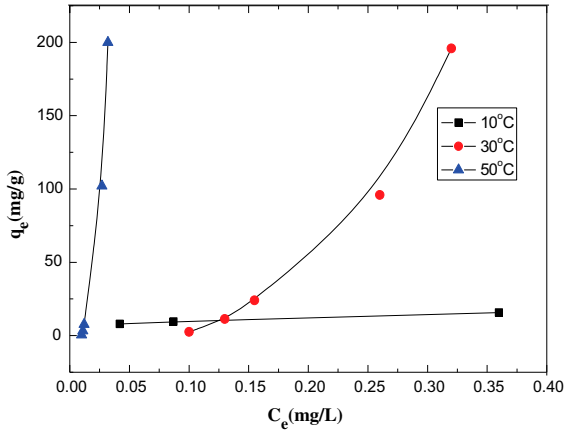

Fig. 8. Effect of temperature on biosorption at pH 4.2, dose 5 g/L, contact time 22 h, and stirring speed 200 rpm.

$$\ln K_C = -\frac{\Delta H^0}{RT} + \frac{\Delta S^0}{R} \quad (4)$$

The values of ΔG^0 obtained were +1.71, -20.22, and -27.79 kJ/mol, respectively, at 10, 30, and 50°C showing an increase in the negative value of ΔG^0 with increase in the temperature which indicated that at higher temperatures, biosorption was more energetically favorable. The standard enthalpy change (ΔH^0) and standard entropy change (ΔS^0) were found to be 211.13 kJ/mol and 0.747 kJ/mol K, respectively. The positive value of ΔH^0 suggested that the process was endothermic in nature and consequently, with increase in temperature the biosorption capacity increased with increased value of K_c. The positive values of ΔS^0 suggested that the biosorbent had high affinity toward Pb(II).

Biosorption isotherms were analyzed by various nonlinear isotherm equations. The model parameters were evaluated by nonlinear regression using Origin 8.5 software. In Table 3, the isotherm constants, coefficient of determination (R^2), and chi-square (χ^2) values for the best-fitted two and three parameter isotherm models are shown. Table 3 indicates that the equilibrium biosorption data at all temperatures were well fitted by the Freundlich and the Khan isotherm at the operating temperatures.

3.5. Effect of contact time

From Fig. 9, it is observed that within the first 2 h the removal of lead was about 88–85% for the initial concentration of 500–1,000 mg/L of lead solution, respectively. After 2 h, biosorption rate became slower and gradually reached equilibrium. About 99.9% of removal was obtained after a contact time of 22 h for both the concentrations. The driving force for the biosorption was the concentration gradient between the available sites for biosorption and available Pb(II) ions. Initially, this concentration gradient was very high leading to a high initial rate of biosorption which decreased thereafter resulting into a slower rate of biosorption [30].

3.6. Desorption study

To study the feasibility of recovery of lead from biosorbent, desorption behavior was observed. Maximum desorption occurred in 0.1 M acetic acid solution. After 30 min about 74% of lead could be desorbed from spent biosorbent containing 199 mg/g of lead. In case of 0.1 M NaCl and 0.1 M $CaCl_2$, only 0.03 and 0.07% of desorption were achieved under similar conditions. The desorption values after 60 min were 60.3, 0.016, and 0.32% for 0.1 M acetic acid, 0.1 M NaCl and 0.1 M $CaCl_2$, respectively. However after 60 min, the desorption (%) remained the same indicating that equilibrium was reached. The reason for maximum desorption in acetic acid was due to formation of bond between loosely bound Pb^{2+} and available acetic acid forming stable lead acetate, which was not possible with NaCl or $CaCl_2$. Complete desorption did not take place as loosely bound Pb^{2+} was not available to react with acetic acid.

Table 3
Isotherm parameters for biosorption of lead at different temperatures

Isotherm model	T (°C)	Model parameters
Freundlich, $q_e = k_F \cdot C_e^{1/n}$	50	$k_F(1\ g^{-1}) = 1.45 \times 10^8$; $n = 0.255$; $R^2 = 0.999$; $\chi^2 = 4.8$
	30	$k_F = 7{,}806$; $n = 0.308$; $R^2 = 0.998$; $\chi^2 = 15.5$
	10	$k_F = 16.88$; $n = 4.72$; $R^2 = 0.988$; $\chi^2 = 9.39$
Khan, $q_e = \frac{q_{m,K} b_K C_e}{(1+b_K C_e)^{a_K}}$	50	$q_{m,K}(mg\ g^{-1}) = 0.211$; $b_K(l\ mg^{-1}) = 98.4$; a_K; $R^2 = 0.999$; $\chi^2 = 6.49$
	30	$q_{m,K} = 1.68$; $b_K = 6.24$; $a_K = -3.7$; $R^2 = 0.998$; $\chi^2 = 16.23$
	10	$q_{m,K} = 15.04$; $b_K = 11.877$; $a_K = 0.836$; $R^2 = 0.992$; $\chi^2 = 6.15$

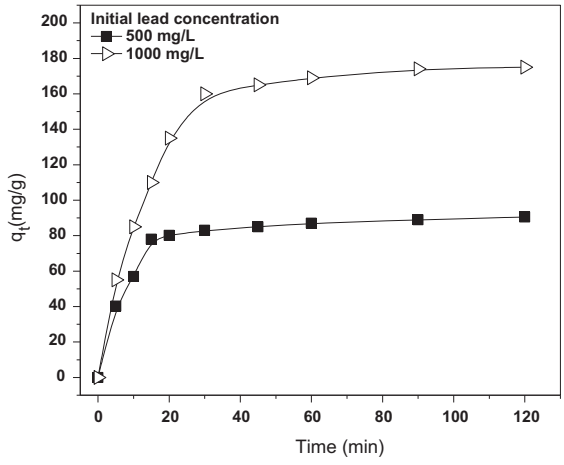

Fig. 9. Effect of contact time on biosorption at an optimized condition of pH 4.2, dose 5 g/L, contact time 2 h, stirring speed 200 rpm, and temperature 30°C.

3.7. Microfiltration study of effluent

Incorporation of microfiltration with the biosorptive treatment resulted in significant improvement in the quality of the treated effluent. Table 4 shows detail characteristics of the effluent at different stages of treatment. It is observed that in the untreated effluent the COD values were about 4,640–5,000 mg/L. The sample contained high amount of oil and grease which was about 2.83–3.37 g/L. Besides, the effluent was rich in ions like lead, phosphorus, sulfate, and zinc. It may be observed that the biosorptive treatment could effectively reduce the lead concentration and in presence of the co-existing ions, the biosorption capacity did not change considerably. Apart from COD and BOD, an enhanced removal of TOC and oil and grease was obtained after microfiltration. TKN was removed due to conversion of organic nitrogen to other forms of nitrogen [31]. The ceramic MF membrane effectively retained the suspended and turbid contaminants in the effluent and turbidity of the permeate samples were < 1 NTU indicating the potential through the process for recycling purpose.

Fig. 10 shows the TOC and COD values of permeate samples during microfiltration of the industrial effluent. In the case of printing industry effluent, generally a significant amount of COD is imparted due to the presence of inorganic materials like photographic and residual chemicals, dyes, hydroxides, organic solvents, and toxic metals contributing toward high COD and TOC [32]. It was observed that the biosorption integrated with MF-based treatment resulted in reduction of COD, as well as TOC. Depending on the feed, TOC value, about 95% reduction of TOC was obtained after 2 h of microfiltration which was greater than COD removal (49%). Organic carbon present in wastewater is composed of different compounds in various oxidation states some of which might be oxidized by biological or chemical processes contributing to the BOD or COD of the sample. However, there are some organic compounds, which may not impart to the BOD or COD values, however, are determined by TOC since TOC measurement is independent of oxidation state of organic matter. This could be interpreted by the experimental observations where the combined process facilitated removal of some organic matters, which could be masked by some interference of compounds in COD measurement and were possibly detected by TOC measurement, resulting in higher TOC removal compared to the COD reduction. Steady state was obtained within 1 h of operation. The values of lead concentration were not changed significantly after microfiltration. However, phosphorus and sulfate were reduced considerably. Overall, in addition to an enhanced removal of lead, the combined process resulted in 98–99% reduction of various associated parameters including TOC, COD, oil and grease, TKN, BOD, turbidity, colour, etc.

Flux profile during microfiltration study of the effluent is shown in Fig. 11. As expected, flux values were increased with increase in the transmembrane pressure and about 219 $Lm^{-2}\ h^{-1}$ of permeation flux

Table 4
Characterization of effluent at different stages of treatment

Parameters	Untreated effluent	Biosorbent treated effluent	Biosorbent + MF treated effluent
pH	2.0–2.5	7.5–7.8	7.6–7.5
COD (mg/L)	4,640–5,000	40–52	20–34
BOD (mg/L)	154–168	32–44	BDL
TOC (mg/L)	574–702	1.0–11.0	0.5–0.6
TKN (%)	2.52–3.0	0.56–0.98	0.2–0.44
TSS (g/L)	9.8–10.7	7.8–8.2	0.022–0.031
Oil and grease (g/L)	2.83–3.37	0.09–0.28	BDL
Turbidity (NTU)	155–167	12–18	0.411–0.675
Colour absorbance (λ_{516} nm)	0.822–0.6778	0.0204–0.0110	0.02–0.01
Conductivity (μS)	5,200–5,000	4,390–4,500	2,200–2,000
TDS (mg/L)	520–560	11.94–13.0	10–11.5
Pb (mg/L)	1,000–1,200	0.037–0.064	0.03–0.052
Zn (mg/L)	2.5–3.6	BDL	BDL
P (mg/L)	4,440–4,660	2,415–2,205	1,577–1,489
SO_4 (mg/L)	66.6–70.5	57.1–48.2	42.2–38.6

Note: BDL—Below detection limit.

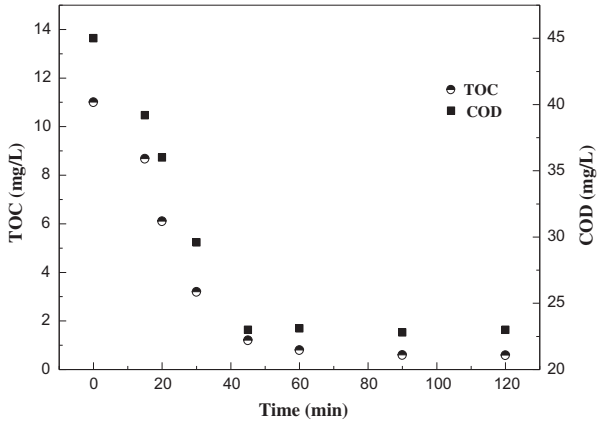

Fig. 10. TOC and COD removal with time during microfiltration study of effluent (feed volume 5 L, time 120 min, TMP 0.098 MPa, and cross-flow velocity 1.6 m/s).

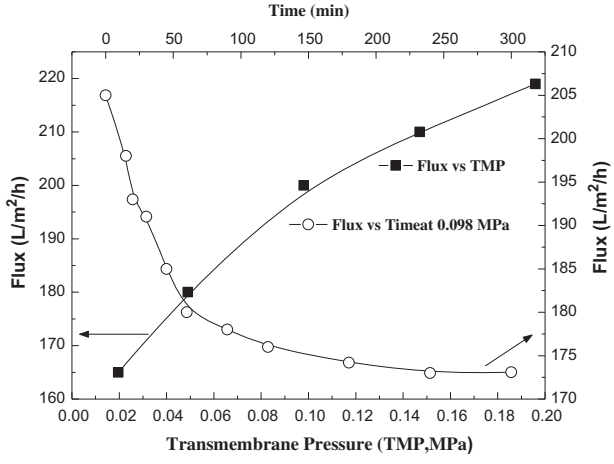

Fig. 11. Effect of time on permeate flux at constant transmembrane pressure of 0.098 MPa and effect of TMP on permeate flux after 20 min during microfiltration study of effluent (feed volume 5 L, crossflow velocity 1.6 m/s).

was observed at an operating pressure of 0.196 MPa with a fixed cross-flow velocity of 1.6 m/s. The constant pressure filtration study at 0.098 MPa indicated that the flux value was almost steady after about 90 min. After 5 h of filtration, flux value was obtained as 173 Lm^{-2} h^{-1} indicating 16% reduction from the initial value.

The FESEM microstructures of indigenously prepared clay-alumina membrane before and after filtration are presented in Fig. 12. From the figure, it is observed that a clear needle-like grain was formed in the membrane with a clear view of pores. But after filtration particles deposited on the membrane surface and hence formed a cake layer. Therefore, after filtration, these needle-like grains of membrane did not appear in the microstructure due to the masking effect of formed layer.

3.8. Reuse study with the treated effluent

Germination (%) of chickpea, soybean, and dried white peas was highest in control followed by that of seeds subjected to permeate effluent treatment. The results are shown in Table 5(a)–(c), respectively, for *Cicer arietinum* L., *Glycine max* (L.) Merr., and *Lathyrus sativus* L. About 90, 83, and 80% germination values

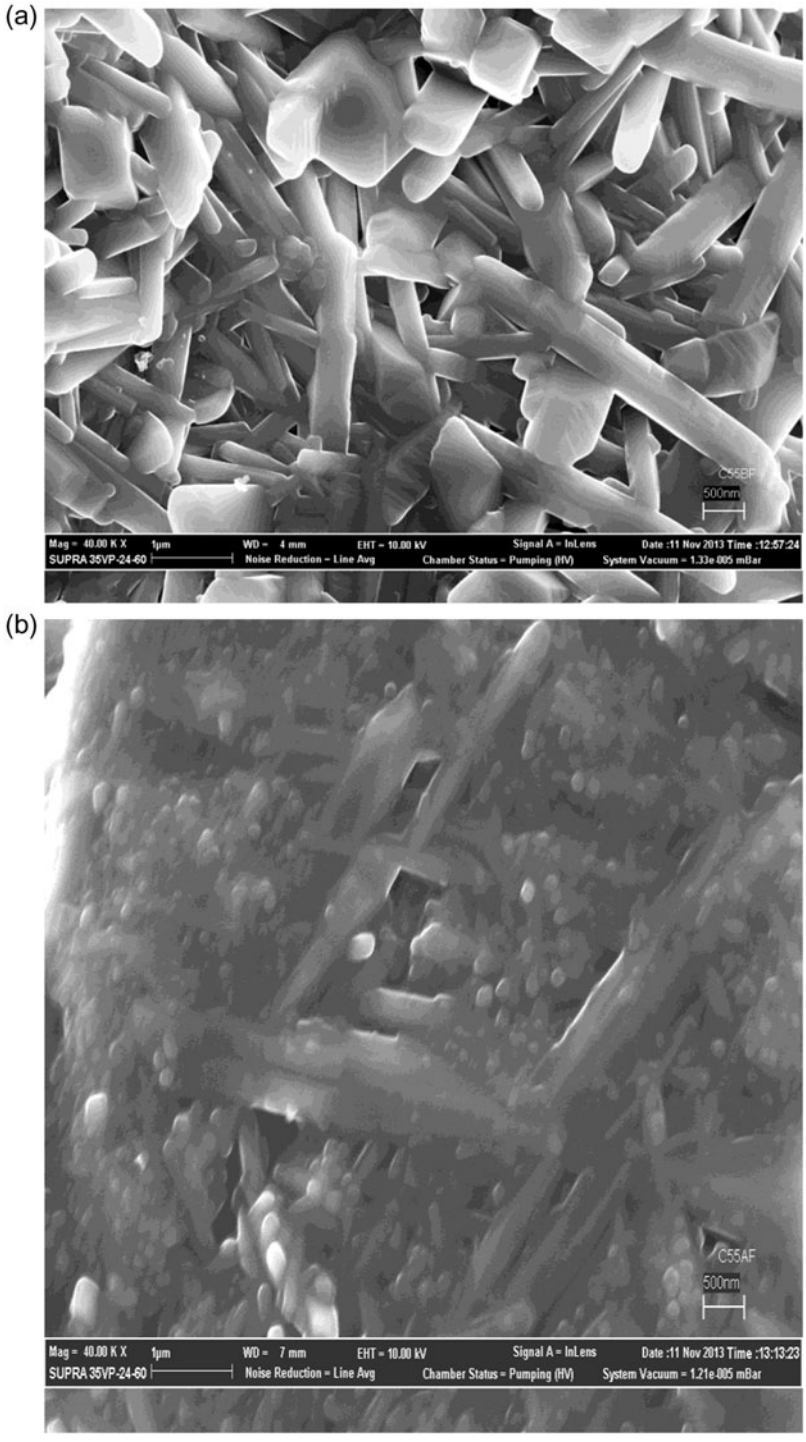

Fig. 12. FESEM image of ceramic membrane. (a) Before use and (b) after use.

were obtained in the case of control for chickpea, soybean, and dried white peas, respectively, whereas in case of seeds exposed to permeate water the rate of germination values was about 83, 73, and 80%, respectively. Decreased rates of germination, about 13, 10, and 13% were obtained for chickpea, soybean, and dried white peas, respectively, exposed to untreated effluent of 25% dilution. Similarly, all other parameters like root length, shoot length, seedling length, seedling vigour index, seedling dry weight, speed of

Table 5
(a) Effect of various treatments on seed quality of *Cicer arietinum* L, (b) Effect of various treatments on seed quality of *Glycine max* (L) Merr, (c) Effect of various treatments on seed quality of *Lathyrus sativus* L

Treatments	Germination (%)	Root length (mm)	Shoot length (mm)	Seedling length (mm)	Seedling vigour index	Seedling dry weight (g/10 seedlings)	Speed of germination	Barlett's germination rate index	First count of germination (%)	Protein content (mg/g)
(a)										
*T*1	90	19.93	14.7	34.68	312.1	0.2844	59.4	0.511	28.88	790
*T*2	83.3	22.7	13.9	36.6	304.9	0.2872	58.1	0.509	28.24	810
*T*3	73.3	12.82	5.6	18.42	135.02	0.2544	38	0.421	11.42	704
*T*4	46.7	9.4	4.3	13.7	63.98	0.2502	24.2	0.376	6.11	520
*T*5	13.3	8.39	0	8.39	11.16	0.2211	11.4	0.214	2.42	430
(b)										
*T*1	83.3	27.2	16.2	43.4	361.52	0.3082	63.7	0.491	27.72	1,472
*T*2	73.3	28.7	15.8	44.5	326.18	0.3004	62.4	0.482	26.44	1,450
*T*3	23.3	22	8.7	30.7	71.53	0.2821	41.2	0.344	8.78	1,270
*T*4	20	9.38	7.1	14.48	28.96	0.2741	26	0.249	5.21	428
*T*5	10	7.78	1.3	9.08	9.08	0.2620	14.5	0.207	1.42	380
(c)										
*T*1	80	26.1	18.8	44.9	359.2	0.2315	57	0.452	23.33	988
*T*2	80	24.5	18.2	42.7	341.6	0.2322	56.5	0.451	25.55	1,072
*T*3	33.3	16.06	12.4	28.46	94.77	0.1944	34.1	0.321	4.88	842
*T*4	30	10.41	11.02	21.43	64.29	0.1721	20	0.304	3.72	838
*T*5	13.3	4.76	0	4.76	6.33	0.1700	7.1	0.271	2.1	672

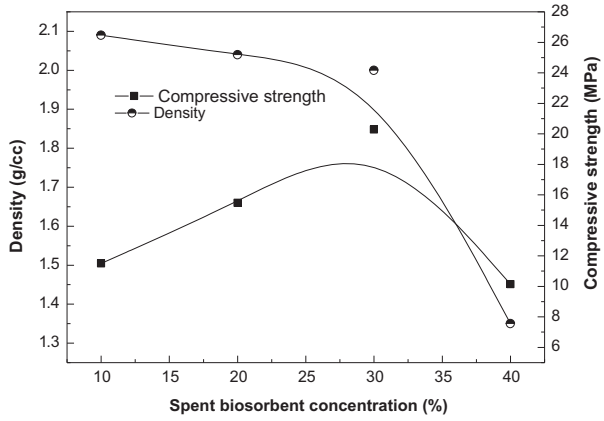

Fig. 13. Effect of spent biosorbent concentration on the density and compressive strength of the clay bricks fired at 1,000°C.

germination, Barlett's germination and first count of germination, and protein content were comparable in case of control- and permeate-treated seeds. In the case of untreated effluent, the values decreased with decreasing dilutions of effluent (Table 5(a) and (c)). Increasing the effluent concentration caused deleterious effect on seed quality parameters. Presence of high lead content in addition to higher COD and BOD values in untreated effluent caused toxic effect on seeds and thereby resulted in decreased germination rate and protein content. Significantly, presence of nutrients in the treated effluent resulted in slight increase of germination rate compared to that of the control. Interestingly protein content of chickpea (~2.5%) and white pea (~7.8%) increased when exposed to permeate water compared to that of control. Hence, it may be concluded that the industrial effluent being effectively detoxified through the proposed treatment process, could potentially be reused towards agricultural or plantation activity.

3.9. Utilization of the spent biosorbent in brick manufacturing

Fig. 13 shows that the spent biosorbent can be used with a concentration of 30% to prepare the bricks since up to this concentration the compressive strength of the bricks increased up to 20.2 MPa. However, above this concentration, the compressive strength decreased significantly. From the figure, it was also observed that the density decreased with increase in spent biosorbent concentration but the reduction in density is significant only after 30%. This reduction in density was, perhaps, due to the burning out of the organic matter of the spent biosorbent. The compressive strength corresponding to 30% addition of spent biosorbent had a good match with the ASTM standard (2006) of grade SW (severe weathering) bricks [33]. After leaching test was performed, the concentrations of Pb, Cr, and Cu in the solution were observed as below the detection limit of AAS for all the samples. Hence, 30% of spent biosorbent could be used safely for the preparation of grade SW bricks.

4. Conclusion

The main conclusions of this comprehensive study are as follows.

The biosorptive treatment in combination with microfiltration involving ceramic membrane has proven successful in complete reuse of heavy metal enriched toxic industrial effluent. The biosorbent prepared from the dried sludge of common effluent treatment plant of tannery shows high potential for removal of toxic lead from synthetic solution as well as industrial effluent. FT-IR, XRD, and XPS characterizations indicate that –COOH and –OH are mostly involved in lead biosorption. The equilibrium isotherm data are well fitted by two-parameter Freundlich model and three-parameter Khan model.

Incorporation of ceramic membrane-based microfiltration process results in an enhanced removal of pollutant load. In addition to 99.99% removal of lead, the combined process is found to be highly effective with about 99.9–99.5% removal of oil and grease, TOC, TKN, BOD, COD, turbidity, and colour. After each washing of the membrane, the flux recovery is around 98.5% without affecting the membrane stability and character.

The treated effluent has a positive effect on seed germination, shoot length, root length, protein content, etc. This is comparable to that of control, which indicates that the combined process may be applied for reuse of industrial effluent for agricultural purpose. The spent biomass generated in the process can be effectively used up to 30% with clay for preparation of bricks with improved mechanical strength. On the whole, the present study proposes a total reuse concept, including an ecofriendly treatment strategy.

Acknowledgment

This study was conducted under the CSIR Network project, ESC0104 under the 12th Five Year Plan funded by the CSIR, Government of India.

References

[1] F.A. Abu Al-Rub, M. Kandah, N. Al-Dabaybeh, Competitive adsorption of nickel and cadmium on sheep manure wastes: Experimental and prediction studies, Sep. Sci. Technol. 38 (2003) 483–497.

[2] S.A. Oke, T.E. Phillips, A. Kolawole, C.E. Ofiabulu, D.A. Adeyeye, Occupational lead exposure in printing presses: An analytical approach, Pacific J. Sci. Technol. 9 (2008) 263–271.

[3] N. Cherry, F. Labreche, J. Collins, T. Tulandi, Occupational exposure to solvents and male infertility, Occup. Environ. Med. 58 (2001) 635–640.

[4] E.L. Thackston, D.J. Wilson, J.S. Hanson, D.L. Miller, Lead removal using adsorption colloidal flotation, Water Pollut. Control Fed. 52 (1980) 317–328.

[5] K. Wilson, H. Yang, C.W. Seo, W.E. Marshall, Select metal adsorption by activated carbon made from peanut shells, Bioresour. Technol. 97 (2006) 2266–2270.

[6] R. Gong, Y. Ding, H. Liu, Q. Chen, Z. Liu, Lead biosorption and desorption by intact and pretreated spirulina maxima biomass, Chemosphere 58 (2005) 125–130.

[7] A. Khosravan, B. Lashkari, Adsorption of Cd(II) by dried activated sludge, Iranian J. Chem. Eng. 8 (2011) 41–56.

[8] S.E. Bailey, T.J. Olin, R.M. Brick, D. Adrian, A review of potentially low-cost sorbents for heavy metals, Water Res. 33 (1999) 2469–2479.

[9] S. Sarkar, S. Bandyopadhyay, A. Larbot, S. Cerneaux, New clay-alumina porous capillary supports for filtration application, J. Membr. Sci. 392–393 (2012) 130–136.

[10] P. Bhattacharya, S. Ghosh, A. Mukhopadhyay, Combination technology of ceramic microfiltration and biosorbent for treatment and reuse of tannery effluent from different streams: Response of defence system in Euphorbia sp., Int. J. Recycling Org. Waste Agric. 2 (19) (2013) 2–19, doi: 10.1186/2251–7715.

[11] P. Bhattacharya, S. Ghosh, S. Swarnakar, A. Mukhopadhyay, Reuse of textile effluent for dyeing using combined technology of ceramic microfiltration and surface treated sugarcane bagasse: Toxicity evaluation using Channa punctatus as model, Desalin. Water Treat. in press, 1–21, doi: 10.1080/19443994.2014.887035.

[12] D.B. Panaskar, R.S. Pawar, Effect of textile mill effluent on growth of *Sorghum vulgare* and *Vigna aconitifolia* seedlings, Indian J. Sci. Technol. 4 (2011) 273–278.

[13] P. Bhattacharya, P. Banerjee, K. Mallick, S. Ghosh, S. Majumdar, A. Mukhopadhyay, S. Bandyopadhyay, Potential of biosorbent developed from fruit peel of *Trewia nudiflora* for removal of hexavalent chromium from synthetic and industrial effluent: Analyzing phytotoxicity in germinating *Vigna* seeds, J. Environ. Sci. Health., Part A. 48 (2013) 706–719.

[14] C.H. Weng, D.F. Lin, P.C. Chiang, Utilization of sludge as brick materials, Adv. Environ. Res. 7 (2003) 679–685.

[15] A.E. Greenberg, A.D. Eaton, L.S. Clesceri, Standard Methods for the Examination of Water and Wastewater, twentyfirst ed., APHA, AWWA, WEF, Washington, DC, 2005.

[16] J. Guo, C. Yang, G. Zen, Treatment of swine wastewater using chemically modified zeolite and bioflocculant from activated sludge, Bioresour. Technol. 143 (2013) 289–297.

[17] A.A. Abul-Baki, J.D. Anderson, Vigor determination in soybean seed by multiple criteria, Crop Sci. 13 (1973) 630–637.

[18] L.E. Evans, G.M. Bhatt, A nondestructive technique for measuring seedling vigor in wheat, Canadian J. Plant Sci. 57 (1977) 983–985.

[19] J.D. Magurie, Speed of germination—Aid in selection and evaluation for seedling emergence and vigor, Crop Sci. 2 (1962) 176–177.

[20] M.S. Bartlett, Some examples of statistical methods of research in agriculture and applied biology (supplement), J. Res. Stat. Soc. 4 (1973) 137–183.

[21] Anonymous, International rules for seed testing, Seed Sci. Technol. 27 (1999) 25–30.

[22] V.G. Panes, P.V. Sukhatme, Statistical Methods for Agriculture Workers, Indian Council of Agricultural Research, New Delhi, 1978.

[23] M.M. Montazer-Rahmati, P. Rabbani, A. Abdolali, A.R. Keshtkar, Kinetics and equilibrium studies on biosorption of cadmium, lead, and nickel ions from aqueous solutions by intact and chemically modified brown algae, J. Hazard. Mater. 185 (2011) 401–407.

[24] J.F. Moulder, W.F. Stickle, P.E. Sobol, K.D. Bomben, Handbook of X-ray Photoelectron Spectroscopy, Perkin-Elmer Corp., Eden Prairie, MN, 1992.

[25] R. Hana, W. Zou, Z. Zhang, J. Shi, J. Yang, Removal of copper(II) and lead(II) from aqueous solution by manganese oxide coated sand I. Characterization and kinetic study, J. Hazard. Mater. 137 (2006) 384–395.

[26] J. Bouanda, L. Dupont, J. Dumonceau, M. Aplincourt, Use of a NICA–Donnan approach for analysis of proton binding to a lignocellulosic substrate extracted from wheat bran, Anal. Bioanal. Chem. 373 (2002) 174–182.

[27] J. Senvaitiene, J. Smirnova, A. Beganskiene, A. Kareiva, XRD and FTIR characterisation of lead oxide-based pigments and glazes, Acta. Chim. Slov. 54 (2007) 185–193.

[28] Y.H. Li, S. Wang, J. Wei, X. Zhang, C. Xu, Z. Luan, D. Wu, B. Wei, Lead adsorption on carbon nanotubes, Chem. Phys. Lett. 357 (2002) 263–266.

[29] W. Xue-jiang, X. Si-quing, C. Ling, Z. Jian-fu, C. Jean-mare, N. Jaffrezie-renault, Biosorption of cadmium (II) and lead (II) ions from aqueous solutions onto dried activated sludge, J. Environ. Sci. 18 (2006) 840–844.

[30] M.A. Al-Anber, Thermodynamics approach in the adsorption of heavy metals, in: J.C.M. Pirajan (Ed.), Thermodynamics–Interaction Studies–Solids, Liquids and Gases, InTech, Rijeka, 2011, pp. 737–764, doi: 10.5772/21326, ISBN: 978-953-307-563-1.

[31] S.A. Al-Jlil, COD and BOD reduction of domestic wastewater using activated sludge, sand filters and activated carbon in Saudi Arabia, Biotechnology 8 (2009) 473–477.

[32] Pollution Prevention and Abatement Handbook, Toward cleaner production/in collaboration with the United Nations Environment Programme and the United Nations Industrial Development Organization, Washington, DC, ISBN 0-8213-3638-X, (1998), pp. 1–441.

[33] Annual Book of ASTM Standards, ASTM International, West Conshohocken, PA, Standard Specification for Building Brick (Solid Masonry Units Made from Clay or Shale), 2006.